Steroids 77 (2012) 212–223

Contents lists available at SciVerse ScienceDirect

Steroids

journal homepage: www.elsevier.com/locate/steroids

Synthesis and biological activities of vitamin D-like inhibitors of CYP24 hydroxylase

Grazia Chiellini [a,b], Simona Rapposelli [c], Jinge Zhu [a], Ilaria Massarelli [d], Marilena Saraceno [c], Anna Maria Bianucci [c,e], Lori A. Plum [a], Margaret Clagett-Dame [a], Hector F. DeLuca [a,*]

[a] Department of Biochemistry, University of Wisconsin-Madison, 433 Babcock Drive, Madison, WI 53706-1544, USA
[b] Dipartimento di Scienze dell'Uomo e dell'Ambiente, Università di Pisa, via Roma 55, 56126 Pisa, Italy
[c] Dipartimento di Scienze Farmaceutiche, Università di Pisa, via Bonanno 6, 56126 Pisa, Italy
[d] Istituto Nazionale per la Scienza e la Tecnologia dei Materiali, via Giusti 9, 50121 Firenze, Italy
[e] International Centre for Studies and Research in Biomedicine (ICB), Luxembourg

ARTICLE INFO

Article history:
Received 10 August 2011
Received in revised form 14 November 2011
Accepted 15 November 2011
Available online 25 November 2011

Keywords:
1,25-Dihydroxyvitamin D_3
Cytochrome P450 inhibitors
CYP24A1
Cyclopropylamines
Cancer therapy
Molecular docking

ABSTRACT

Selective inhibitors of CYP24A1 represent an important synthetic target in a search for novel vitamin D compounds of therapeutic value. In the present work, we show the synthesis and biological properties of two novel side chain modified 2-methylene-19-nor-1,25$(OH)_2D_3$ analogs, the 22-imidazole-1-yl derivative **2** (VIMI) and the 25-*N*-cyclopropylamine compound **3** (CPA1), which were efficiently prepared in convergent syntheses utilizing the Lythgoe type Horner–Wittig olefination reaction. When tested in a cell-free assay, both compounds were found to be potent competitive inhibitors of CYP24A1, with the cyclopropylamine analog **3** exhibiting an 80–1 selective inhibition of CYP24A1 over CYP27B1. Addition of **3** to a mouse osteoblast culture sustained the level of 1,25$(OH)_2D_3$, further demonstrating its effectiveness in CYP24A1 inhibition. Importantly, the *in vitro* effects on human promyeloid leukemia (HL-60) cell differentiation by **3** were nearly identical to those of 1,25$(OH)_2D_3$ and *in vivo* the compound showed low calcemic activity. Finally, the results of preliminary theoretical studies provide useful insights to rationalize the ability of analog **3** to selectively inhibit the cytochrome P450 isoform CYP24A1.

1. Introduction

The hormonal form of vitamin D_3, 1α,25-dihydroxyvitamin D_3 (1,25$(OH)_2D_3$, **1**) (Fig. 1) has long been known for its central role in controlling calcium and phosphate homeostasis. In addition, a growing body of investigations is continuously unveiling the significance of vitamin D in a diverse array of physiological functions, including cell proliferation, differentiation and apoptosis, and immune response. Consequently, vitamin D deficiency has been associated with a number of diseases such as cancers, autoimmune dysfunctions, cardiovascular diseases, and infections [1–3]. As the therapeutic activity of exogenously administered 1,25$(OH)_2D_3$ is limited by its capacity to induce hypercalcemia, numerous efforts have been directed to develop therapeutically useful 1,25$(OH)_2D_3$ analogs. Although many of them have resulted in useful therapies, in particular for the treatment of kidney, bone and skin diseases [4,5], their use in other areas remains nonexistent primarily due to the difficulty of achieving an effective concentration without also raising serum calcium.

Vitamin D_3, the natural form of vitamin D produced in the skin through UV exposure, is biologically inert. Activation of vitamin D_3 is initiated in the liver to produce 25-hydroxyvitamin D_3 (25$(OH)D_3$), which is further converted to 1α,25-dihydroxyvitamin D_3 (1,25$(OH)_2D_3$), the hormonally active secosteroid, by 25$(OH)D_3$ 1α-hydroxylase (CYP27B1) mainly in the kidney. Metabolic inactivation of 1,25$(OH)_2D_3$ in its target cells is initiated by side chain hydroxylations at the C-23, C-24, and C-26 positions. Of these hydroxylation sites, it is now accepted that the sequential oxidation and cleavage of the side chain by mitochondrial 1,25$(OH)_2D_3$ 24-hydroxylase (CYP24A1) (Fig. 2) is the major pathway by which the hormone is inactivated [6]. CYP24A1, as the main catabolizing enzyme of 1,25$(OH)_2D_3$, can also break down vitamin D analogs in a similar catabolic process. Elevated CYP24A1 levels have been seen in many types of human cancers [7], immune dysfunctions, and secondary hyperparathyroidism. In addition, intervention with vitamin D analogs often stimulates the expression of CYP24A1, resulting in rapid elimination of the active metabolites, that drastically reduces the effectiveness of the treatment. Targeting CYP24 provides the opportunity to increase endogenous levels of 1,25$(OH)_2D_3$, or reduce the effective dose of exogenous 1,25$(OH)_2D_3$. Conventional drug design approaches have led to the development of a range of P450 inhibitors that are currently used in the clinic, primarily as antifungal agents. Effective inhibitors can be found in a class of bifunctional lipophilic compounds (entitled azoles) that directly link to the heme iron by the azole nitrogen and, additionally, interact with

* Corresponding author. Tel.: +1 608 262 1620; fax: +1 608 262 7122.
E-mail address: deluca@bioChem.wisc.edu (H.F. DeLuca).

0039-128X/$ - see front matter © 2011 Elsevier Inc. All rights reserved.
doi:10.1016/j.steroids.2011.11.007

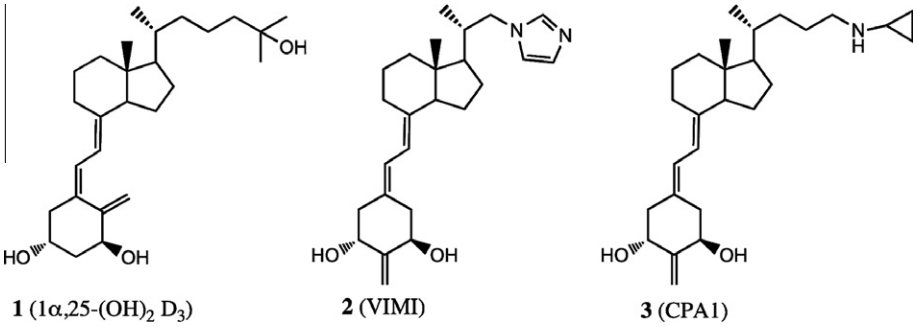

Fig. 1. Chemical structures of 1α,25-dihydroxyvitamin-D_3 and new designed CYP24 inhibitors.

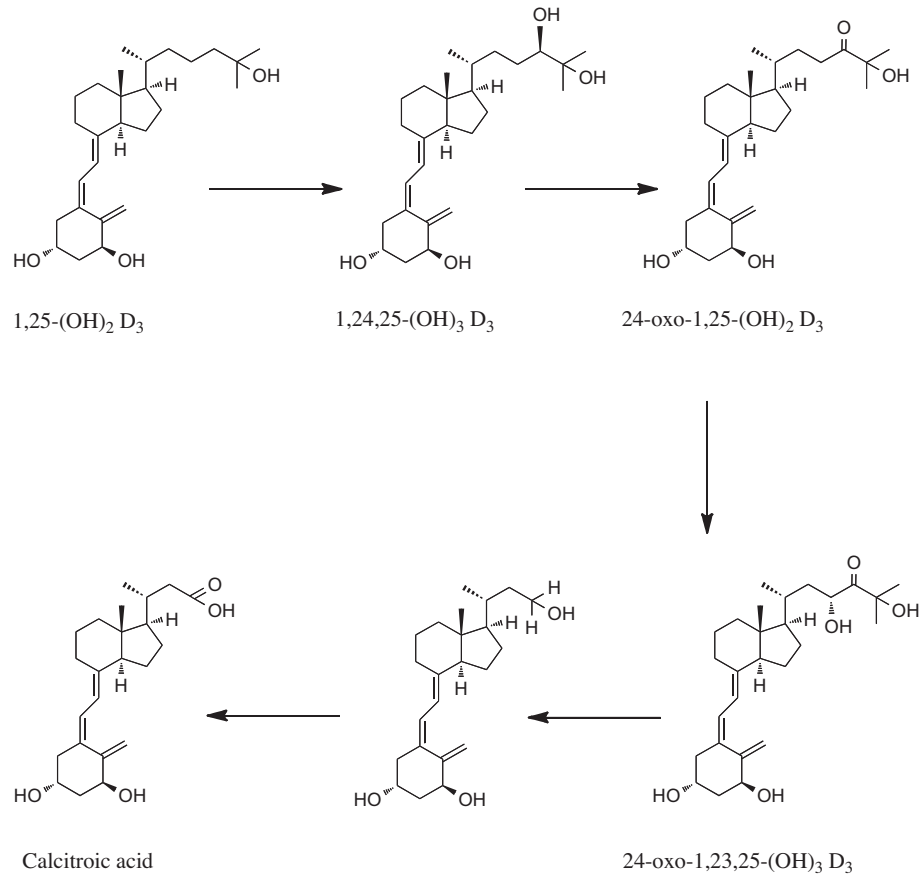

Fig. 2. CYP24A1 oxidation pathway.

other parts of the substrate site. Currently, the non-selective CYP inhibitor ketoconazole (Fig. 3) has been shown to inhibit CYP24 and act synergistically with vitamin D analogs in cell cultures [8] and is being tried in combination with Calcitriol in a phase I clinical trial [9]. Liarazole (Fig. 3) has also been shown to inhibit 1,25$(OH)_2D_3$ hydroxylation and act synergistically with 1,25$(OH)_2D_3$ in androgen independent DU-145 prostate cancer cells [10]. However, a major problem of many azole inhibitors is their low selectivity.

Due to these limitations, selective CYP24 inhibitors offer a therapeutic advantage, and several groups have developed compounds to this end [11–16]. Aiming at increased/sustained hormone levels, a project to develop azole-type inhibitors of CYP24A1 was started in Novartis in the early 1990s. More than 400 structurally different azole-type compounds were tested, using primary human keratinocytes as model system. A compound termed VID 400 (Fig. 3) showed the desired qualities as a strong selective CYP24A1 inhibitor, and was chosen for development in the indication of psoriasis [11,12]. Simons' group reported CYP24A1 inhibitory activity of tetralone derivatives and *N*-[2-(1*H*-imidazol-1-yl)-2-phenylethyl] arylamides, but their selectivity has not been assessed [13,14]. C-24 analogs of 1,25$(OH)_2D_3$ licensed to Cytochroma Inc. and termed "vitamin D signal amplifiers" are both, potent inhibitors of CYP24A1 and agonists of the vitamin D signaling pathway. The lead compound CTA018, where C24 is replaced with a sulfoximine functional group [15,16] (Fig. 3), is at the beginning of clinical Phase II in the indication: topical treatment of mild to moderate psoriasis.

Cyclopropylamine derivatives are also known to have interesting and sometimes useful properties as enzyme inhibitors [17]. Since the initial reports that *N*-benzyl-*N*-cyclopropylamine

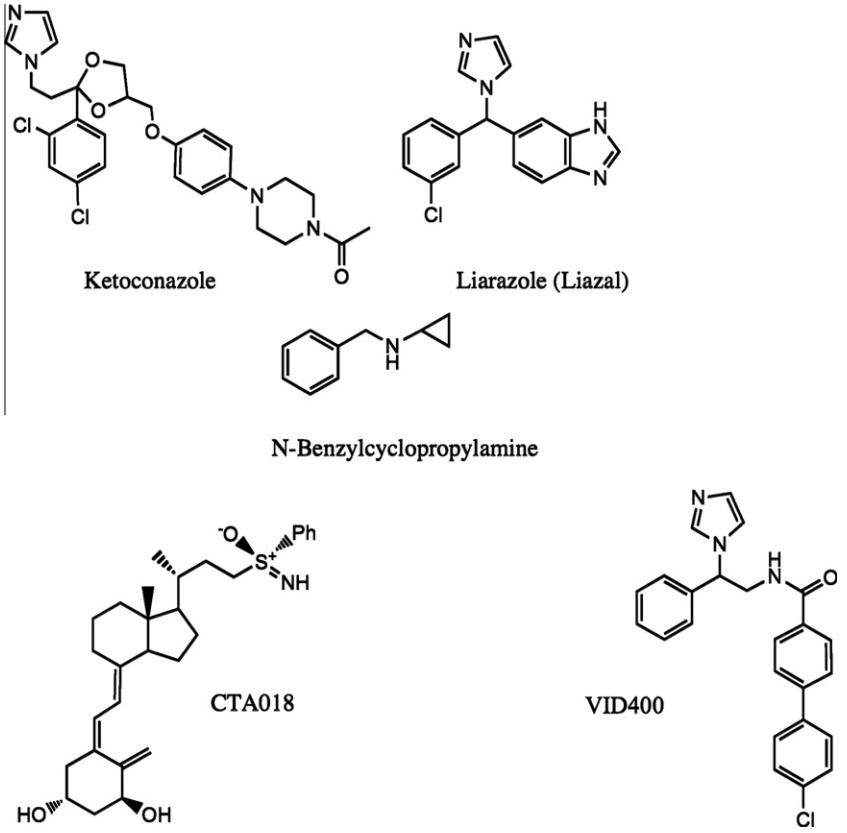

Fig. 3. Chemical structures of cytochrome P450 inhibitors.

(Fig. 3) is a suicide substrate for cytochrome P450 enzymes, as well as for monoamine oxidase, cyclopropylamines have been widely applied as mechanistic probes of these and other oxidative enzymes. The cyclopropylamine substructure is indeed found in several biologically active natural products and is increasingly found within synthetic drug and drug candidate molecules [18–24].

Based on these findings, we decided to prepare two novel vitamin D-like analogs having an azole group **2** (VIMI) or a cyclopropylamine moiety **3** (CPA1) on the modified side chain (Fig. 1). Interestingly, both these new compounds turned out to be potent inhibitors of CYP24A1, with **3** showing specific inhibition of CYP24A1 over CYP27B1. Although the azole analog **2** displayed a very low potency as a vitamin D analog, the cyclopropylamine compound **3** was found to induce HL-60 cells differentiation with the same potency as $1,25(OH)_2D_3$, while showing lower potency in raising calcium tissue levels. Therefore this novel analog may ultimately be useful as a new and safer therapeutic agent. A molecular docking study provided useful insights to rationalize the ability of analog **3** to selectively inhibit the cytochrome P450 isoform CYP24A1 and to optimize the lead structure to obtain compounds suitable to enter the pre-clinical and clinical drug development programs.

2. Experimental procedures

2.1. General

Optical rotations were measured in chloroform or methanol using a Perkin–Elmer model 343 polarimeter at 22 °C. Ultraviolet (UV) absorption spectra were recorded with a Perkin–Elmer Lambda 3B UV–Vis spectrophotometer in ethanol. ^{1}H nuclear magnetic resonance (NMR) spectra were recorded in deuteriochloroform, acetone-d_6, or methanol-d_4 at 400 and 500 MHz with Bruker Instruments DMX-400 and DMX-500 Avance console spectrometers. ^{13}C NMR spectra were recorded in deuteriochloroform, at 100 and 125 MHz with the same Bruker Instruments. Chemical shifts (δ) in parts per million are quoted relative to internal Me_4Si (δ 0.00). Electron impact (EI) mass spectra were obtained with a Micromass AutoSpec (Beverly, MA) instrument. HPLC was performed on a Waters Associates liquid chromatograph equipped with a model 6000A solvent delivery system, model U6K Universal injector, and model 486 tunable absorbance detector. THF was freshly distilled before use from sodium benzophenone ketyl under argon. A designation "(volume + volume)", which appears in general procedures, refers to an original volume plus a rinse volume.

Both final vitamin D analogs synthesized by us gave single sharp peaks on HPLC, and they were judged at least 99.5% pure. The purity and identity of the synthesized vitamins were additionally confirmed by inspection of their ^{1}H NMR, ^{13}C NMR, UV absorption, and high-resolution mass spectra.

2.2. Synthesis of compounds

2.2.1. (8S,20S)-des-A,B-20-(1′-methylimidazolyl)-pregnan-8-ol (7)

A solution of diol **5** [25] (0.50 g, 2.35 mmol) in anhydrous pyridine (5 mL) was cooled to −25 °C. A precooled solution of tosyl chloride (0.55 g, 2.90 mmol) in anhydrous pyridine (1 mL) was added dropwise to the diol solution via cannula. Upon stirring for 3.5 h at −25 °C, the reaction was warmed to 0 °C and allowed to stir for an additional 20 h. The mixture was extracted with CH_2Cl_2, washed with saturated $CuSO_4$ aqueous solution, dried ($MgSO_4$), filtered, and concentrated to give a residue which was chromatographed on a silica gel column with hexane/ethyl acetate (8:2) to afford 0.60 g (1.68 mmol) of the corresponding tosylate **6** in 70% yield. To a solution of imidazole (0.046 g, 0.67 mmol) in dry DMF (5 mL) at 0 °C under argon was added NaH (60% dispersion in oil,

0.057 g, 1.42 mmol), and the mixture was stirred at the same temperature for 20 min. A solution of tosylate **6** (0.12 g, 0.34 mmol) in dry DMF (3 mL) was added dropwise over 15 min. The reaction mixture was warmed to room temperature, and after being stirred for 24 h at room temperature, the mixture was quenched with water and extracted with EtOAc. The organic phase was dried and evaporated, and the residue was purified by flash chromatography. Gradient elution (1–5% MeOH/$CHCl_3$) afforded 0.085 g (0.32 mmol) of **7** in 95% yield as a white solid. $[\alpha]_D$ +28.7° (*c* 1.25, CH_2Cl_2); ^{1}H NMR ($CDCl_3$, 400 MHz) δ 7.42 (s, 1H), 7.05 (s, 1H), 6.87 (s, 1H), 4.11 (d, *J* = 2.3 Hz, 1H), 4.01 (dd, *J* = 13.7, 3.6 Hz, 1H), 3.54 (dd, *J* = 13.7, 9.2 Hz, 1H), 0.98 (s, 3H), 0.84 (d, *J* = 6.6 Hz, 3H); ^{13}C NMR ($CDCl_3$, 100.6 MHz) δ, 137.7, 129.1, 119.4, 68.9, 54.2, 52.7, 52.3, 42.1, 40.1, 38.0, 33.6, 27.3, 22.6, 17.3, 16.9, 13.5; exact mass calculated for $C_{16}H_{26}N_2O$ (M^+) 262.2040, found 262.2050.

*2.2.2. (20S)-des-A,B-8–20-(1′-methylimidazolyl)-pregnan-8-one (**4**)*

Molecular sieves A4 (0.4 nm, 4 Å) (0.15 g) were added to a solution of 4-methylmorpholine (0.074 g, 0.63 mmol) in dichloromethane (3 mL). The mixture was stirred at room temperature for 15 min and tetrapropylammoniumperruthenate (TPAP) (2 mg, 0.006 mmol) was added, followed by a solution of alcohol **7** (0.02 g, 0.076 mmol) in dichloromethane (1 mL). The resulting suspension was stirred at room temperature for 1 h. The reaction mixture was filtered through a Waters silica Sep-Pack cartridge (5 g) that was further washed with ethyl acetate/2-propanol (10:1). After removal of the solvent the ketone **4** (0.015 g, 77% yield) was obtained as a colorless oil. ^{1}H NMR ($CDCl_3$, 400 MHz) δ 7.44 (s, 1H), 7.07 (s, 1H), 6.88 (s, 1H), 4.03 (dd, *J* = 13.8, 3.6 Hz, 1H), 3.54 (dd, *J* = 13.8, 9.0 Hz, 1H), 0.90 (d, *J* = 6.6 Hz, 3H), 0.69 (s, 3H); ^{13}C NMR ($CDCl_3$, 100.6 MHz) δ, 211.3, 137.7, 129.3, 119.4, 61.5, 54.1, 52.5, 49.8, 40.8, 38.7, 38.1, 27.6, 23.8, 19.2, 17.3, 12.5; exact mass calculated for $C_{16}H_{24}N_2O$ $(M)^+$ 260.1884, found 260.1885.

*2.2.3. (8S,20S)-de-A,B-8-triethylsilyloxy-20-(acetyloxymethyl) pregnane (**8**)*

Acetic anhydride (0.41 g, 0.40 mL, 4.0 mmol) was added to a solution of the diol **5** (0.5 g, 2.3 mmol) and Et_3N (1.64 mL, 11.7 mmol) in anhydrous CH_2Cl_2 (20 mL) at room temperature (rt). The reaction mixture was stirred at rt for 24 h, diluted with methylene chloride (100 mL), washed with 5% aq. HCl, water, saturated aq. $NaHCO_3$, dried (Na_2SO_4) and concentrated under reduced pressure. The residue (0.68 g) was chromatographed on silica gel with hexane/ethyl acetate (75:25) to give the desired alcohol (0.53 g, 88% yield) as a colorless oil.

To a stirred solution of the alcohol (0.53 g, 2.1 mmol) and 2,6-lutidine (0.29 mL, 0.26 g, 2.5 mmol) in anhydrous methylene chloride (5 mL) triethylsilyl trifluoromethane-sulfonate (0.54 mL, 2.5 mmol) was added at 0 °C. The reaction mixture was allowed to warm to room temperature (1 h), and stirring was continued for additional 30 min. Methylene chloride was added and the mixture was washed with water, dried (Na_2SO_4) and concentrated under reduced pressure. The residue was chromatographed on silica gel with hexane/ethyl acetate (97:3) to afford the protected diol **8** (0.74 g, 95% yield) as a colorless oil: $[\alpha]_D$ +40.77 (*c* 4.9, $CHCl_3$); ^{1}H NMR (400 MHz, $CDCl_3$) δ 4.06 (2H, m), 3.77 (1H, dd, *J* = 10.6, 3.1 Hz, 22-H), 2.05 (3H, s), 1.93 (1H, br. d, *J* = 12.4 Hz), 0.98 (3H, d, *J* = 6.6 Hz, 21-H_3), 0.96 (9H, t, *J* = 7.9 Hz), 0.92 (3H, s), 0.56 (6H, q, *J* = 7.9 Hz); ^{13}C NMR (100 MHz) δ, 171.4, 69.6, 69.2, 53.4, 52.8, 42.3, 40.6, 35.4, 34.6, 26.8, 23.1, 21.0, 17.7, 17.1,13.6, 6.9, 5.0; exact mass calculated for $C_{19}H_{35}O_3Si$ ($M-C_2H_5$) 339.2355, found 339.2347.

*2.2.4. (8S,20S)-de-A,B-8-triethylsilyloxy-20-(hydroxymethyl) pregnane (**9**)*

The protected diol **8** (0.58 g, 1.6 mmol) was then treated with a solution of NaOH (1 g, 25 mmol) in anhydrous ethanol (20 mL) at room temperature. After stirring of the reaction mixture for 3 h, ice and 5% aq. HCl were added until pH 6. The solution was extracted with ethyl acetate (3 × 50 mL) and the combined organic phases were washed with saturated aq. $NaHCO_3$, dried (Na_2SO_4) and concentrated under reduced pressure. The residue was chromatographed on silica gel with hexane/ethyl acetate (75:25) to give the alcohol **9** (0.44 g, 84% yield) as a colorless oil.

$[\alpha]_D$ +41.1 (*c* 2.85, $CHCl_3$); ^{1}H NMR (400 MHz, $CDCl_3$ + TMS) δ 4.04 (1H, d, *J* = 2.4 Hz, 8α-H), 3.63 (1H, dd, *J* = 10.5, 3.2 Hz, 22-H), 3.38 (1H, dd, *J* = 10.5, 6.8 Hz, 22-H), 1.94 (1H, br. d, *J* = 12.4 Hz), 1.02 (3H, d, *J* = 6.6 Hz, 21-H3), 0.95 (9H, t, *J* = 7.9 Hz), 0.92 (3H, s, 18-H_3), 0.55 (6H, q, *J* = 7.9 Hz); ^{13}C NMR (100 MHz) δ, 69.2, 67.9, 53.1, 52.8, 42.1, 40.6, 38.3, 34.6, 26.8, 23.0, 17.6, 16.6, 13.5, 6.9, 4.9; exact mass calculated for $C_{19}H_{38}O_2Si$ (M^+) 326.2641, found 326.2626.

*2.2.5. (8S,20S)-de-A,B-8-triethylsilyloxy-20-formylpregnane (**10**)*

To a solution of oxalyl chloride (1.11 g, 8.74 mmol) in DMSO (1.2 mL) at −60 °C, a solution of the primary alcohol **9** (0.22 g, 0.67 mmol) in anhydrous CH_2Cl_2 (2 mL) at −60 °C was added via cannula. The resulting mixture was stirred at −60 °C for 2 h, quenched with Et_3N (4.9 mL), and warmed up to room temperature. Upon dilution with H_2O, the mixture was extracted with CH_2Cl_2, dried ($MgSO_4$), filtered, concentrated, and purified by flash column chromatography (95:5 hexane/ethyl acetate; R_f = 0.12) to give the desired aldehyde **10** (0.120 mg, 0.37 mmol, 54% yield) as an oil.

^{1}H NMR (200 MHz, $CDCl_3$) δ 9.57 (1H, d, *J* = 3.0 Hz, CHO), 4.06 (1H, d, *J* = 2.4 Hz, 8α-H), 2.38 (1H, m, 20-H), 1.09 (3H, d, *J* = 6.8 Hz, 21-H_3), 0.95 (12H, m, Si(CH_2CH_3)$_3$ + 18-H_3), 0.55 (6H, q, *J* = 7.8 Hz, Si(CH_2CH_3)$_3$).

*2.2.6. (8S,20S)-de-A,B-8-triethylsilyloxy-20-[2-(methoxycarbonyl)-et-(1E)-en-yl] pregnane (**11**)*

To a solution of the aldehyde **10** (0.120 g, 0.37 mmol) in absolute EtOH (3 mL) at 0 °C was added methyl(triphenylphosphoranylidene)-acetate (0.307 g, 0.92 mmol) and Et_3N (0.037 g, 0.37 mmol). The mixture was stirred at rt for 24 h and then the solvent was evaporated. The residue was purified by flash column chromatography (95:5 hexane/ethyl acetate, R_f = 0.45) to obtain **11** (0.105 g, 0.27 mmol, 75% yield) as an oil.

$[\alpha]_D$ +58.5 (*c* 2.37, CH_2Cl_2); ^{1}H NMR (400 MHz, $CDCl_3$ + TMS) δ 6.83 (1H, dd, *J* = 15.1, 9.0 Hz), 5.73 (1H, d, *J* = 15.6 Hz), 4.03 (1H, d, *J* = 2.4 Hz, 8α-H), 3.76 (3H, s) 1.94 (1H, br. d, *J* = 12.4 Hz), 1.05 (3H, d, *J* = 6.6 Hz, 21-H3), 0.95 (12H, m), 0.55 (6H, q, *J* = 7.9 Hz); ^{13}C NMR (100 MHz) δ, 167.6, 155.3, 118.4, 69.2, 55.5, 52.9, 51.3, 42.4, 40.6, 39.4, 34.6, 27.3, 23.0, 19.1, 17.6, 13.8, 6.9, 4.9; exact mass calculated for $C_{20}H_{36}O_3Si$ (M^+–Et) 351.2350, found 351.2366.

*2.2.7. (8S,20R)-de-A,B-8-triethylsilyloxy-20-(hydroxypropyl) pregnane (**12**)*

A solution of the compound **11** (0.105 g, 0.27 mmol) in absolute EtOH (5 mL) was hydrogenated for 9 h in the presence of 10% palladium on powdered charcoal (15 mg). The reaction mixture was filtered through a bed of Celite with several ethanol washes, the filtrate was concentrated and the residue was chromatographed on silica gel with hexane/ethyl acetate (97:3, R_f = 0.47) to give the saturated ester (0.092 g, 0.24 mmol, 89% yield), which after dissolving in THF (1 mL) was immediately exposed to reduction with $LiAlH_4$ 1 M in THF (0.48 mL, 0.48 mmol) at −10 °C. The reaction mixture was stirred at rt for 3 h, then water (0.2 mL) and NaOH 1 M (0.05 mL) were added, and the resulting suspension was filtered. The evaporation of the solvent afforded the alcohol **12** (0.070 g, 0.20 mmol, 82% yield) as a clear oil.

^{1}H NMR (400 MHz, $CDCl_3$ + TMS) δ 4.03 (1H, d, *J* = 2.4 Hz, 8α-H), 3.62 (2H, m) 1.96 (1H, br. d, *J* = 12.4 Hz), 0.99–0.90 (15H, m), 0.55 (6H, q, *J* = 7.9 Hz); ^{13}C NMR (100 MHz) δ, 69.4, 63.7, 56.7 53.1, 42.1,

40.8, 35.1, 34.6, 31.7, 29.7, 27.3, 23.0, 18.6, 17.7, 13.5, 6.9, 4.9; exact mass calculated for $C_{21}H_{42}O_2Si$ (M^+) 354.2949, found 354.2943.

2.2.8. (8S,20R)-de-A,B-8-triethylsilyloxy-20-[3-(cyclopropylamine) propyl] pregnane (**14**)

To a solution of oxalyl chloride (0.34 g, 2.91 mmol) in DMSO (1.2 mL) at −60 °C a solution of the primary alcohol **12** (0.081 g, 0.23 mmol) in anhydrous CH_2Cl_2 (2 mL) was added via cannula. The resulting mixture was stirred at −60 °C for 2 h, quenched with Et_3N (4.9 mL), and warmed up to room temperature. Upon dilution with H_2O, the mixture was extracted with CH_2Cl_2, dried ($MgSO_4$), filtered, concentrated, and purified by flash column chromatography (95:5 hexane/ethyl acetate; R_f = 0.55) to give the desired aldehyde **13** (0.046 g, 0.13 mmol, 57% yield) which was immediately used for the next step. ^{1}H NMR (200 MHz, $CDCl_3$) δ 9.76 (1H, s, CHO), 4.02 (1H, br. signal, 8α-H), 2.40 (2H, m, 23-H_2), 0.94 (15H, m, $Si(CH_2CH_3)_3$ + 18-H_3 + 21-H_3), 0.54 (6H, q, J = 8.0 Hz, $Si(CH_2CH_3)_3$).

To a solution of the aldehyde **13** (0.046 g, 0.13 mmol) in anhydrous CH_2Cl_2 (1 mL) was added cyclopropylamine (0.0092 g, 0.16 mmol) and the mixture was cooled at 0 °C before adding sodium triacetoxyborohydride (0.047 g, 0.22 mmol). The reaction mixture was stirred at rt for 2 h. Then sat. aq. $NaHCO_3$ solution (1 mL) was added and the mixture was extracted with EtOAc. The organic phase was dried ($MgSO_4$), filtered, and the solvent was evaporated to give **14** (0.049 g, 0.12 mmol, 95% yield).

$[\alpha]_D$ +44.5 (*c* 1.12, CH_2Cl_2); ^{1}H NMR (400 MHz, $CDCl_3$ + TMS) δ 4.02 (1H, d, J = 2.4 Hz, 8α-H), 2.65 (2H, m), 2.13 (1H, m), 0.95 (9H, t, J = 7.9 Hz), 0.89 (6H, m), 0.55 (6H, q, J = 7.9 Hz), 0.43 (2H, m), 0.36 (2H, m); ^{13}C NMR (100 MHz) δ, 69.4, 56.7, 53.1, 50.2, 42.1, 40.8, 35.2, 34.6, 33.4, 30.3, 27.3, 26.4, 23.0 18.6, 17.7, 13.5, 6.9, 6.2, 6.1, 4.9; exact mass calculated for $C_{24}H_{48}NOSi$ ($M+H^+$) 394.3505, found 394.3506.

2.2.9. (8S,20R)-de-A,B-20-[3-(cyclopropyl-N-t-Boc-amine) propyl] pregnan-8-ol (**15**)

To a solution of compound **14** (0.033 g, 0.084 mmol) in CH_3CN (3 mL) Boc_2O (0.022 g, 0.10 mmol) and DMAP (0.001 g, 0.0084 mmol) were added under vigorous stirring. After stirring at rt for 1 h, the mixture was diluted with EtOAc, washed with water and brine then dried ($MgSO_4$). Concentration gave the desired protected amine (0.040 g, 0.081 mmol, 96% yield). ^{1}H NMR (400 MHz, $CDCl_3$ + TMS) δ 4.02 (1H, d, J = 2.4 Hz, 8α-H), 3.14 (2H, m), 2.49 (1H, m), 1.95 (1H, br. d, J = 12.4 Hz), 1.46 (9H, s), 0.94 (9H, t, J = 7.9 Hz), 0.89 (6H, m), 0.73 (2H, m), 0.56 (8H, m).

Removal of the TES was achieved by treating the protected alcohol (0.032 g, 0.065 mmol) dissolved in anhydrous THF (5 mL) with TBAF 1 M in THF (130 mL, 0.13 mmol). After 5 h of stirring at rt the reaction mixture was diluted with EtOAc, washed with brine, dried ($MgSO_4$) and concentrated under reduced pressure. The residue was purified by flash column chromatography on silica gel with hexane/ethyl acetate (95:5) to give the alcohol **15** (0.016 g, 0.042 mmol, 65% yield). ^{1}H NMR (400 MHz, $CDCl_3$ + TMS) δ 4.07 (1H, s, 8α-H), 3.14 (2H, m), 2.48 (1H, m), 1.98 (1H, br. d, J = 12.4 Hz), 1.46 (9H, s), 0.93 (3H, s), 0.91 (6H, m), 0.73 (2H, m), 0.57 (2H, m).

2.2.10. (8S,20R)-de-A,B-20-[3-(cyclopropyl-N-t-Boc-amine)propyl] pregnan-8-one (**16**)

Pyridinium dichromate (PDC) (0.079 g, 0.211 mmol) was added to a solution of the alcohol **15** (0.016 g, 0.042 mmol) and pyridinium *p*-toluenesulfonate (PPTS) (0.007 g, 0.030 mmol) in anhydrous CH_2Cl_2 (5 mL). The resulting suspension was stirred at rt for 3 h. The reaction mixture was filtered through a Waters silica Sep-Pack cartridge (5 g) that was further washed with hexane/ethyl acetate (95:5). After removal of the solvent the ketone **16** (0.014 g, 0.037 mmol, 88% yield) was recovered as a colorless oil.

^{1}H NMR (400 MHz, $CDCl_3$ + TMS) δ 3.15 (2H, m), 2.45 (2H, m), 1.46 (9H, s), 0.96 (3H, d, J = 5.7 Hz), 0.73 (2H, m), 0.64 (3H, s), 0.58 (2H, m); ^{13}C NMR (100 MHz) δ, 212.1, 156.8, 79.2, 61.9, 56.6, 49.9, 40.9, 47.8, 38.9, 35.3, 32.8, 28.5, 27.5, 24.8, 24.0, 19.0, 18.7, 12.5, 8.0, exact mass calculated for $C_{23}H_{39}NO_3Na$ ($M+Na^+$) 400.2823, found 400.2821.

2.2.11. (20S)-2-methylene-22-(imidazol-1-yl)-19,23,24,25,26,27-esanor-1α-hydroxyvitamin D_3 (**2**)

To a solution of phosphine oxide **17** [26] (0.107 g, 0.184 mmol) in anhydrous THF (0.4 mL) at −20 °C was slowly added PhLi (1.8 M in di-*n*-butylether, 0.129 mL, 0.232 mmol) under argon with stirring. The solution turned deep orange. After 30 min the mixture was cooled to −78 °C and a precooled (−78 °C) solution of ketone **4** (0.015 g, 0.058 mmol) in anhydrous THF (0.2 + 0.1 mL) was slowly added. The mixture was stirred under argon at −78 °C for 3 h and at 0 °C for 18 h. Ethyl acetate was added, and the organic phase was washed with brine, dried (Na_2SO_4) and evaporated. The residue was dissolved in hexane and applied on a Waters silica Sep-Pack cartridge (2 g). The cartridge was washed with hexane and hexane/ethyl acetate (90:10) to give 19-norvitamin derivative **18** (0.023 g, 63% yield). Then the Sep-Pack was washed with ethyl acetate to recover diphenylphosphine oxide **17** (0.06 g). For analytical purpose a sample of protected vitamin **18** was further purified by HPLC (9.4 × 2.50 mm Zorbax Sil column, 4 mL/min, hexane/2-propanol/TEA (94:6:0.5) solvent system, RT = 11.09 min).

^{1}H NMR ($CDCl_3$, 800 MHz) δ 7.43 (s, 1H), 7.05 (s, 1H), 6.88 (s, 1H), 6.21 (d, J = 11.2 Hz, 1H), 5.86 (d, J = 11.2 Hz, 1H), 4.99 (s, 1H), 4.93 (s, 1H), 4.44 (m, 2H), 4.05 (dd, J = 13.6, 4.0 Hz, 1H), 3.57 (dd, J = 13.6, 8.8 Hz, 1H), 2.85 (dm, J = 12.8 Hz, 1H), 2.54 (dd, J = 13.6, 5.6 Hz, 1H), 2.48 (dd, J = 12.8, 4.0 Hz, 1H), 2.35 (dd, J = 13.6, 3.2 Hz, 1H), 2.20 (dd, J = 2.8, 8.0. Hz, 1H), 0.92 (s, 9H), 0.89 (s, 9H), 0.86 (d, J = 6.4 Hz, 3H), 0.61 (s, 3H), 0.10 (s, 3H) 0.096 (s, 3H), 0.073 (s, 3H), 0.055 (s, 3H); ^{13}C NMR ($CDCl_3$, 200.9 MHz) δ 153.1, 140.5, 137.8, 133.5, 129.4, 122.4, 119.7, 116.8, 106.6, 72.7, 71.8, 56.2, 54.3, 53.0, 47.8, 46.0, 40.5, 39.1, 38.8, 28.8, 28.0, 26.0, 23.5, 22.6, 18.5, 18.4, 17.4, 14.4, 12.3, −4.6, −4.9; exact mass calculated for $C_{37}H_{65}N_2O_2Si_2$ (MH)$^+$ 625.4580, found 625.4570.

The protected vitamin **18** (0.023 g, 0.037 mmol) was dissolved in acetonitrile (2 mL). A solution of aq. 48% HF in acetonitrile (1:9 ratio, 2 mL) was added at 0 °C and the resulting mixture was stirred at room temperature for 8 h. Saturated aq. $NaHCO_3$ solution was added and the reaction mixture was extracted with ethyl acetate. The combined organic phases were washed with brine, dried (Na_2SO_4) and concentrated under reduced pressure. The residue was diluted with 2 mL of hexane/ethyl acetate (3:1) and applied on a Waters silica Sep-Pack cartridge (2 g). An elution with ethyl acetate/hexane (1:1) and later with ethylacetate/2-propanol (10:1) gave the crude product **2** (0.014 g). The vitamin **2** was further purified by normal phase HPLC [9.4 × 250 mm Zorbax Sil column, 4 mL/min, hexane/2-propanol/TEA (74:25:1) solvent system, RT = 7.74 min] to give a colorless oil (0.012 g, 80% yield).

UV (in EtOH) λ_{max} 261.0, 251.5, 244.0 nm; ^{1}H NMR ($CDCl_3$, 800 MHz) δ 7.42 (s, 1H), 7.03 (s, 1H), 6.86 (s, 1H), 6.33 (d, J = 11.2 Hz, 1H), 5.89 (d, J = 11.2 Hz, 1H), 5.10 (s, 1H), 5.08 (s, 1H), 4.47 (m, 2H), 4.02 (dd, J = 13.6, 4.0 Hz, 1H), 3.56 (dd, J = 13.6, 8.8 Hz, 1H), 2.85 (dd, J = 13.6, 4.8 Hz, 1H), 2.82 (dm, J = 12.8, 4.8 Hz, 1H), 2.57 (dd, J = 13.6, 4.0 Hz, 1H), 2.33 (dd, J = 13.6, 6.4 Hz, 1H), 2.29 (dd, J = 12.8, 8.0. Hz, 1H), 0.86 (d, J = 6.4 Hz, 3H), 0.60 (s, 3H); ^{13}C NMR ($CDCl_3$, 200.9 MHz) δ, 152.2, 142.5, 137.9, 131.4, 129.3, 124.1, 119.7, 116.0, 108.0 72.0, 70.8, 56.2, 54.3, 53.0, 46.1, 46.0, 40.4, 39.0, 38.4, 29.0, 28.0, 23.5, 22.7, 17.4, 12.4; exact mass calculated for $C_{25}H_{37}N_2O_2$ [MH]$^+$ 397.2850, found 397.2851.

*2.2.12. N-cyclopropyl-(20R)-2-methylene-19,25,26,27-tetranor-25-aza-1α-hydroxyvitamin D (**3**)*

To a solution of phosphine oxide **17** (0.086 g, 0.148 mmol) in anhydrous THF (0.5 mL) at −20 °C was slowly added PhLi (1.7 M in di-*n*-butylether, 0.087 mL, 0.148 mmol) under argon with stirring. The solution turned deep orange. After 30 min the mixture was cooled at −78 °C and a precooled (−78 °C) solution of ketone **16** (0.014 g, 0.037 mmol) in anhydrous THF (0.2 + 0.1 mL) was slowly added. The mixture was stirred under argon at −78 °C for 3 h and at 0 °C for 18 h. Ethyl acetate was added, and the organic phase was washed with brine, dried ($MgSO_4$) and evaporated. The residue was dissolved in hexane and applied on a Waters silica Sep-Pack cartridge (2 g). The cartridge was washed with hexane and hexane/ethyl acetate (99.5:0.5) to give the 19-norvitamin **19** (0.021 g, 0.028 mmol, 76% yield).

^{1}H NMR ($CDCl_3$, 900 MHz) δ 6.20 (1H, d, J = 10.8 Hz), 5.82 (1H, d, J = 10.8 Hz,), 4.96 (1H, s,), 4.91 (1H, s,), 4.41 (2H, m), 3.15 (2H, m), 2.81 (1H, dm, J = 12.6 Hz), 2.52 (1H dd, J = 13.5, 6.3 Hz), 2.45 (1H, dd, J = 12.6, 4.5 Hz), 2.32 (1H, dd, J = 13.5, 2.7 Hz), 2.17 (1H, dd, J = 12.6, 8.1. Hz), 1.46 (9H, s), 0.94 (3H, d, J = 7.2 Hz), 0.89 (9H, s), 0.86 (9H, s), 0.73 (2H, m), 0.58 (2H, m), 0.54 (3H, s) 0.098 (3H, s) 0.096 (3H, s), 0.073 (3H, s), 0.055 (3H, s); ^{13}C NMR ($CDCl_3$, 200.9 MHz) δ 157.0, 153.2, 141.4, 133.0, 122.6, 116.4, 106.5, 72.7, 71.8, 56.7, 56.5, 47.8, 45.9, 40.8, 38.8, 36.1, 33.2, 29.0, 28.7, 27.9, 26.1, 23.6, 22.4, 19.0, 18.5, 18.4, 12.3, 8.5, −4.6, −4.9; exact mass calculated for $C_{44}H_{79}NO_4Si_2Na$ $(MNa)^+$ 764.5440, found 764.5469.

The protected vitamin **19** (0.021 g, 0.028 mmol) was dissolved in THF (2 mL) and CH_3CN (2 mL). A solution of aq. 48% HF in CH_3CN (1:9 ratio, 2 mL) was added at 0 °C and the resulting mixture was stirred at rt for 8 h. Saturated aq. $NaHCO_3$ solution was added and the reaction mixture was extracted with ethyl acetate. The combined organic phases were washed with brine, dried ($MgSO_4$) and concentrated under reduced pressure. The residue was chromatographed on silica gel ethyl acetate/hexane (80:20) to give the desired final product **3** (0.008 g, 0.019 mmol, 69% yield). The vitamin **3** was further purified by HPLC (9.4 × 250 mm Zorbax Sil column, 4 mL/min, hexane/2-propanol (80:20) solvent system, RT = 8.50 min). UV (in EtOH) λ_{max} 261.0, 251.5, 244.0 nm; ^{1}H NMR ($CDCl_3$, 400 MHz) δ 6.35 (1H, d, J = 11.2 Hz), 5.88 (1H, d, J = 11.2 Hz), 5.11 (1H, s), 5.09 (1H, s), 4.62 (2H, m), 2.87–2.80 (2H, m), 2.70–2.55 (3H, m), 2.35–2.26 (2H, m), 2.12 (1H, m), 0.93 (3H, d, J = 6.3 Hz), 0.55 (3H, s), 0.42 (2H, m), 0.34 (2H, m); ^{13}C NMR ($CDCl_3$, 100 MHz) δ, 152.0, 143.4, 130.4, 124.2, 115.3, 107.7, 71.8, 70.6, 56.4, 56.3, 50.2, 45.8, 40.4, 38.2, 36.0, 33.5, 30.4, 28.9, 27.7, 26.6, 24.7, 23.5, 22.3, 18.8, 12.1, 6.2; exact mass calculated for $C_{27}H_{44}NO_2$ $(MH)^+$ 413.3289, found 413.3297.

2.3. Biology

2.3.1. CYP24A1 inhibition assay

Assay reactions were performed in a buffer containing 20 mM Tris (pH 7.5), 125 mM NaCl, 0.1 μM adrenodoxin (Adx), 0.1 μM adrenodoxin reductase (AdR), 0.075 μM CYP24A1, varying concentrations of $1,25(OH)_2D_3$ (1.25–2.50 μM) and inhibitors, and 0.5 mM NADPH. The reactions were conducted and analyzed by HPLC as previously reported [27]. The K_i values were determined by fitting the relative activity (V/V_0) against the inhibitor concentration [I] using the equation $V/V_0 = (K_M + [S])/[K_M(1 + [I]/K_i) + [S]]$, where V and V_0 are the reaction rates in the presence and absence of inhibitors, respectively.

2.3.2. CYP27B1 inhibition assay

Inhibition of CYP27B1 [27] was assayed in a manner similar to that of CYP24A1 as described above except that the buffer contained 20 mM Tris (pH 7.5), 125 mM NaCl, 0.1% CHAPS, 2 μM Adx, 0.2 μM AdR, 0.025 μM CYP27B1, various amounts of $25(OH)D_3$ (1.25–2.50 μM) and inhibitors, and 1.0 mM NADPH. The HPLC mobile phase was in 7% 2-propanol in hexane.

2.3.3. Determination of the $1,25(OH)_2D_3$ half-life

Primary mouse osteoblasts were isolated from fetal calvaria and cultured to 70% confluency in αMEM containing 10% FBS in 24-well plates (1 mL/well). Two days later, the culture was treated with 2.5 nM or 2.5 pM $1,25(OH)_2D_3$ and a trace amount of [^{3}H]-$1,25(OH)_2D_3$ in the presence and absence of 1 μM ketoconazole or 1 μM **3**. At various time points (0, 8, 24, and 48 h), 200 μL of medium was withdrawn and extracted with 800 μL of dichloromethane twice. The organic phase was dried down and separated via HPLC in 15% 2-propanol in hexane as described above. The residual [^{3}H]-$1,25(OH)_2D_3$ in the medium over a 48 h period was quantitated by counting the tritium.

2.3.4. In vitro studies

VDR binding, CYP24A1 transcription, and HL-60 differentiation assays were performed as previously described [28].

2.3.5. In vivo studies

Bone calcium mobilization and intestinal calcium transport were performed as previously described [28]. Briefly, weanling rats were made vitamin D-deficient by housing under lighting conditions that block vitamin D production in the skin. In addition, the animals were fed a diet devoid of vitamin D and alternating levels of calcium. Experimental compounds were administered intraperitoneally once per day for four consecutive days. Twenty-four hours after the last dose was given, the blood was collected, and everted gut sacs were prepared. Calcium was measured in the blood and two different intestinal compartments using atomic absorption spectrometry. Each study was comprised of at least 5–6 animals/experimental group and was controlled with a vehicle group (5% ethanol:95% propylene glycol) and one or more positive control groups [$1,25(OH)_2D_3$].

2.4. Docking studies

The 3D structure of the human CYP24A1 was built with swisspdbviewer [29] thanks to its homology to the crystal structure of the rat isoform (ID: 3K9V), which was obtained from PDB [30] and taken as template structure. The homology based modeling protocol relied on a sequence alignment, obtained from the web server Blast [31] (as shown in Fig. 4). The alignment score revealed a sequence similarity of 83%, which ensured that a reliable model for the human isoform could be obtained.

The sequence of the human isoform was loaded in swisspdbviewer together with the 3D structure of the crystallized rat isoform (3K9V). The alignment, shown in Fig. 4, enabled automatic building of a model for the human CYP24A1, which was then refined within the swisspdbviewer software. A theoretical model for the human CYP27B1 isoform was downloaded from the MODBASE server [32].

Molecular docking was then accomplished by means of the molecular docking software, AutoDock version 4.0 [33]. The polar hydrogens and united atom Kollman charges were assigned to the enzymes during the preparation of the protein input files, containing fragmental volume and solvation parameters. For the ligands and the heme group, partial atomic charges were determined by the Gasteiger method with modification to ensure unit charge on each residue. Moreover, rotatable bonds were assigned with AutoDock Tools, an accessory program that allows the user to interact with AutoDock from a graphic user interface. Prior to the AutoDock, AutoGrid was exploited for the preparation of the grid map using a grid box with a npts (number of points in *xyz*) of 50–60–50 Å which defines the simulation space. The box

```
 Score =  899 bits (2322),  Expect = 0.0, Method: Compositional matrix adjust.
 Identities = 427/514 (83%), Positives = 465/514 (90%), Gaps = 0/514 (0%)

Query  1    MSCPIDKRRTLIAFLRRLRDLGQPPRSVTSKASASRAPKEVPLCPLMTDGETRNVTSLPG  60
            MS PI K R+L AFL++LR   QPPR VTS A  S  P+EVP+CPL   GET+N  +LPG
Sbjct  1    MSSPISKSRSLAAFLQQLRSPRQPPRLVTSTAYTSPQPREVPVCPLTAGGETQNAAALPG  60

Query  61   PTNWPLLGSLLEIFWKGGLKKQHDTLAEYHKKYGQIFRMKLGSFDSVHLGSPSLLEALYR  120
            PT+WPLLGSLL+I WKGGLKKQHDTL EYHKKYG+IFRMKLGSF+SVHLGSP LLEALYR
Sbjct  61   PTSWPLLGSLLQILWKGGLKKQHDTLVEYHKKYGKIFRMKLGSFESVHLGSPCLLEALYR  120

Query  121  TESAHPQRLEIKPWKAYRDHRNEAYGLMILEGQEWQRVRSAFQKKLMKPVEIMKLDKKIN  180
            TESA+PQRLEIKPWKAYRD+R E YGL+ILEG++WQRVRSAFQKKLMKP E+MKLD KIN
Sbjct  121  TESAYPQRLEIKPWKAYRDYRKEGYGLLILEGEDWQRVRSAFQKKLMKPGEVMKLDNKIN  180

Query  181  EVLADFLERMDELCDERGRIPDLYSELNKWSFESICLVLYEKRFGLLQKETEEEALTFIT  240
            EVLADF+ R+DELCDERG + DLYSELNKWSFESICLVLYEKRFGLLQK   +EA+ FI
Sbjct  181  EVLADFMGRIDELCDERGHVEDLYSELNKWSFESICLVLYEKRFGLLQKNAGDEAVNFIM  240

Query  241  AIKTMMSTFGKMMVTPVELHKRLNTKVWQAHTLAWDTIFKSVKPCIDNRLQRYSQQPGAD  300
            AIKTMMSTFG+MMVTPVELHK LNTKVWQ HTLAWDTIFKSVK CIDNRL++YSQQP AD
Sbjct  241  AIKTMMSTFGRMMVTPVELHKSLNTKVWQDHTLAWDTIFKSVKACIDNRLEKYSQQPSAD  300

Query  301  FLCDIYQQDHLSKKELYAAVTELQLAAVETTANSLMWILYNLSRNPQAQRRLLQEVQSVL  360
            FLCDIY Q+ LSKKELYAAVTELQLAAVETTANSLMWILYNLSRNPQ Q++LL+E+QSVL
Sbjct  301  FLCDIYHQNRLSKKELYAAVTELQLAAVETTANSLMWILYNLSRNPQVQQKLLKEIQSVL  360

Query  361  PDNQTPRAEDLRNMPYLKACLKESMRLTPSVPFTTRTLDKPTVLGEYALPKGTVLTLNTQ  420
            P+NQ PRAEDLRNMPYLKACLKESMRLTPSVPFTTRTLDK TVLGEYALPKGTVL LNTQ
Sbjct  361  PENQVPRAEDLRNMPYLKACLKESMRLTPSVPFTTRTLDKATVLGEYALPKGTVLMLNTQ  420

Query  421  VLGSSEDNFEDSHKFRPERWLQKEKKINPFAHLPFGIGKRMCIGRRLAELQLHLALCWII  480
            VLGSSEDNFEDS +FRPERWLQ+++KINPFAHLPFG+GKRMCIGRRLAELQLHLALCWI+
Sbjct  421  VLGSSEDNFEDSSQFRPERWLQEKEKINPFAHLPFGVGKRMCIGRRLAELQLHLALCWIV  480

Query  481  QKYDIVATDNEPVEMLHLGILVPSRELPIAFRPR  514
            +KYDI ATDNEPVEMLH G LVPSRELPIAF  R
Sbjct  481  RKYDIQATDNEPVEMLHSGTLVPSRELPIAFCQR  514
```

Fig. 4. Alignment between rat and human CYP24A1 sequences. Query: CYP24A1 human, Sbjct: CYP24A1 rat.

spacing was 0.375 Å and the grid was set in order to cover the entire space of the binding site. A distance-dependent function of the dielectric constant was used for the calculation of the energetic maps. AutoDock was run using the maximum number of energy evaluation retries and generations, 10,000 and 27,000, respectively. The Lamarckian genetic algorithm (LGA) with the pseudo-Solis and Wets modification (LGA/pSW) method was used with default parameters for calculation of the docking possibilities [34].

3. Results

3.1. Chemistry

The synthetic strategy for new analogs **2** and **3** was based on the Lythgoe type Horner–Wittig olefination reaction [26], which has been extensively utilized by us for the preparation of a large number of vitamin D compounds [25,35]. This approach required using two specific Grundmann-type ketones **4** (Scheme 1) and **16** (Scheme 2), which we prepared from the known diol **5**, obtained in our laboratory from commercial vitamin D_2 [25]. Selective tosylation of the primary hydroxy group of diol **5** provided the corresponding tosylate **6** (Scheme 1), which after addition of the sodium salt of imidazole in dry DMF, gave the imidazole alcohol **7** in 95% yields. Catalytic oxidation of the secondary alcohol with tetrapropylammonium perruthenate [36] in the presence of 4-methylmorpholine *N*-oxide afforded the expected ketone **4** in very good yields. In order to obtain the CD-ring ketone **16** we prepared the aldehyde **10** starting from the diol **5** (Scheme 2). The Wittig reaction between aldehyde **10** and methyl (triphenylphosphoranylidene)-acetate provided the olefinic product **11** that after catalytic hydrogenation followed by $LiAlH_4$ reduction furnished the primary alcohol **12**. Then, Swern oxidation [37] provided the aldehyde **13** that after reaction with cyclopropylamine and reduction of the resulting Schiff base with triacetoxyborohydride provided the CD-ring cyclopropylamine side chain modified intermediate **14**. After protection of the secondary amino group as a *t*-butyl (BOC)

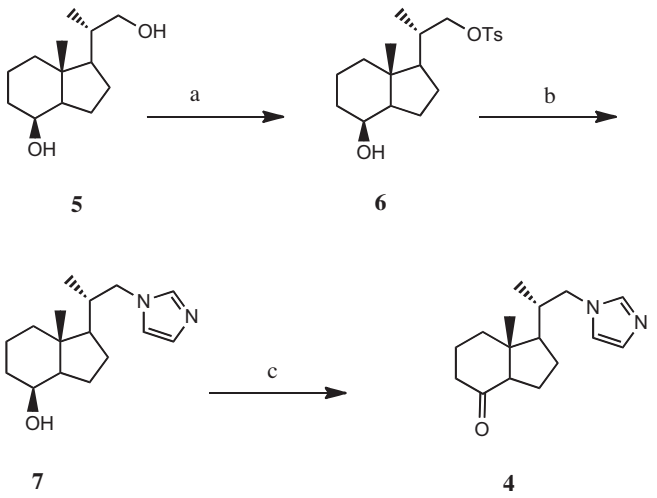

Scheme 1. Synthesis of ketone **4**. *Reagents and conditions:* (a) TsCl/pyridine/−25 °C. (b) Imidazole/NaH/DMF/0 °C. (c) TPAP/NMO/molecular sieves/rt.

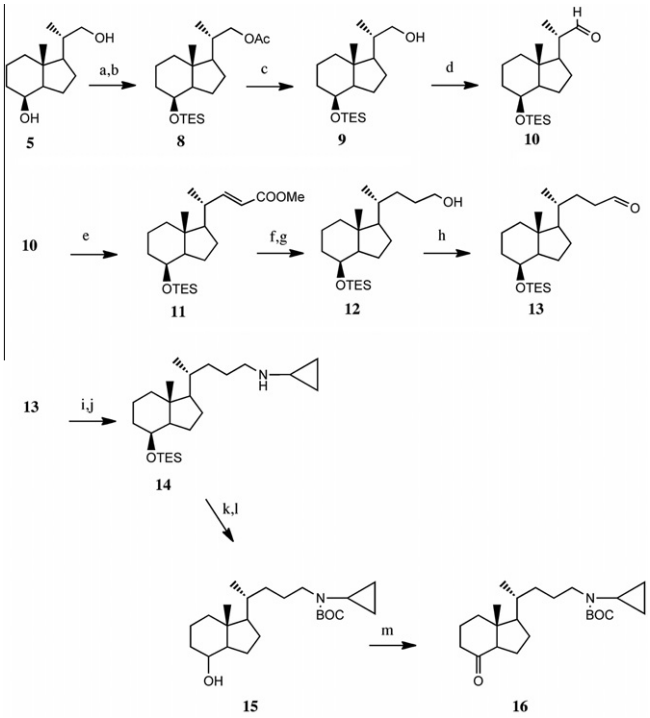

Scheme 2. Synthesis of ketone **15**. *Reagents and conditions:* (a) Ac_2O/Et_3N/rt. (b) TESOTf/ 2,6-lutidine/CH_2Cl_2/0 °C. (c) NaOH/EtOH/rt. (d) $C_2O_2Cl_2$/DMSO/CH_2Cl_2/−60 °C. (e) Ph_3P = CHCOOMe/EtOH/Et_3N/0 °C. (f) H_2/Pd–C/EtOH/rt. (g) $LiAlH_4$/THF/−10 °C. (h) $C_2O_2Cl_2$/DMSO/CH_2Cl_2/−60 °C. (i) cyclopropylamine/CH_2Cl_2/rt. (j) $Na(OAc)_3BH$/0 °C. (k) Boc_2O/DMAP/CH_3CN/rt. (l) TBAF/THF/rt. (m) PDC/CH_2Cl_2/rt.

carbamate followed by selective cleavage of the triethylsilyl protecting group treating with tetrabutylammonium fluoride (nBu$_4$N$^+$F$^-$, TBAF) the secondary alcohol **15**, was obtained. Oxidation of alcohol **15** with pyridinium dichromate afforded the desired CD-ring ketone **16** (Scheme 2). As shown in Scheme 3 the Horner–Wittig reaction between the corresponding C,D-fragments **4** and **16** and the anion, generated from the phosphine oxide **17** by phenyllithium [38], produced the protected vitamin D compounds **18**–**19**. The silyl-protective groups as well as the *t*-butyl (BOC) carbamate were cleaved in the presence of hydrofluoric acid and after the final purification by HPLC the target vitamin D analogs **2** (VIMI) and **3** (CPA1) were obtained.

3.2. Biological evaluation

3.2.1. Inhibition of CYP24A1 and CYP27B1

Since current assays for CYP24A1 inhibition rely on the use of different preparations (e.g., primary human keratinocyte culture,

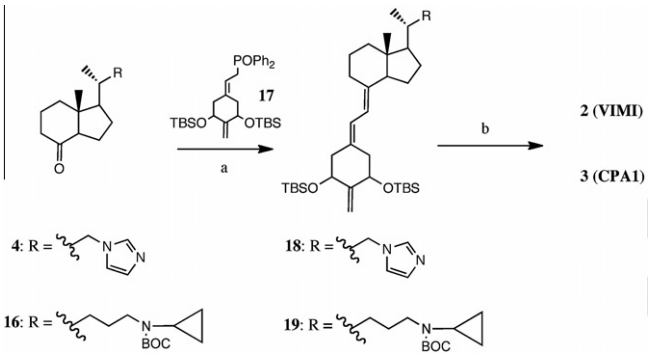

Scheme 3. Synthesis of 2-methylene-19-nor-1,25(OH)$_2$D$_3$ analogs **2** and **3**. *Reagents and conditions:* (a) PhLi/THF/−78 °C. (b) Aqueous HF/THF/MeCN/rt.

Table 1
Inhibition constants of vitamin D analogs toward CYP24A1 and CYP27B1.

Inhibitor	K_i (μM)		
	CYP24A1	CYP27B1	Selectivity
2	0.021 ± 0.007	0.090 ± 0.017	4.3
3	0.042 ± 0.014	3.34 ± 0.38	80
Ketoconazole	0.032 ± 0.005	0.053 ± 0.010	1.6

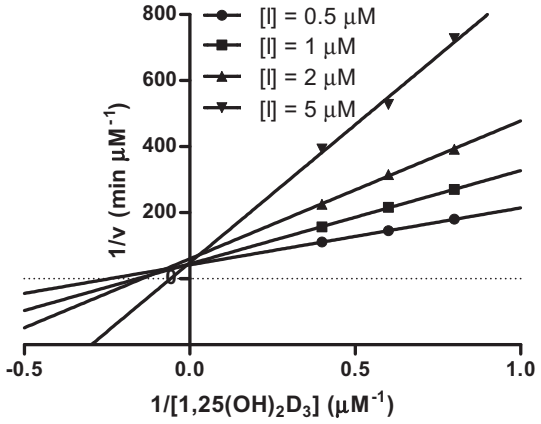

Fig. 5. Lineweaver–Burke plot showing competitive inhibition of CYP24A1 by analog **3** (CPA1).

recombinant hamster cell line, or rat kidney mitochondria) and consequently suffer from experimental variability in enzyme content and the presence of physiological partners and other interacting factors, we recently developed a simple, clean, and sensitive enzymatic assay [27]. In short, variants of human CYP24A1 proteins, with a C-terminal His tag or an N-terminal fusion to maltose binding protein (MBP), were overexpressed in *Escherichia coli* and purified to apparent homogeneity. The hydroxylase activity was reconstituted *in vitro*, and the resulting cell-free assay system was applied in the screening of **2**, **3** and other vitamin D analogs synthesized in our laboratory. Additional assays were also performed to measure their inhibitory activity towards CYP27B1 [27]. As shown in Table 1, **2** and **3** along with ketoconazole exhibited potent inhibition of CYP24A1, with K_i values ranging from 0.021 μM (VIMI) to 0.042 μM (CPA1). Ketoconazole, which had a

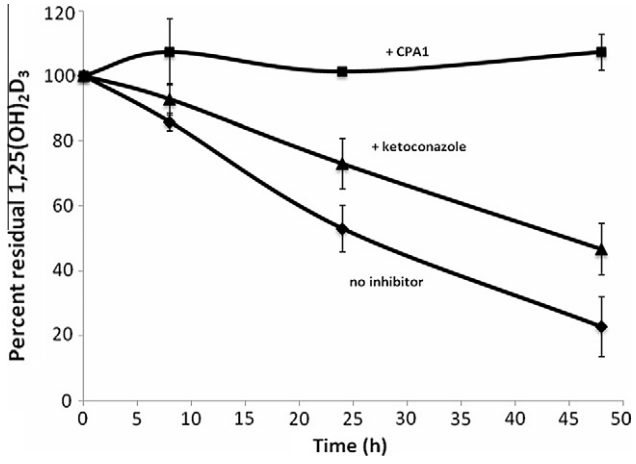

Fig. 6. Time course of residual 1,25(OH)$_2$D$_3$ in the medium of the mouse osteoblast culture in the presence and absence of CYP24A1 inhibitors. Each value is a mean ± SD of three determinations.

Table 2
VDR binding properties. Transcriptional activities, and HL-60 differentiation activities of **2** (VIMI) and **3** (CPA1), in comparison to those of **1** ($1,25(OH)_2D_3$).

	VDR binding		CYP24A1 transcription		HL-60 differentiation	
	K_i (M)	Ratio	EC_{50} (M)	Ratio	EC_{50} (M)	Ratio
1	2×10^{-11}	1	2×10^{-10}	1	2×10^{-9}	1
2	7×10^{-8}	3500	$>10^{-6}$	>5000	$>10^{-6}$	>500
3	3×10^{-9}	150	3×10^{-9}	15	8×10^{-9}	4

K_i value of 0.032 μM toward CYP24A1, was equally effective at suppressing CYP27B1 activity, with a K_i value of 0.053 μM. This was also true with **2**, which showed only a moderate selectivity of 4.3 for inhibition of CYP24A1 over CYP27B1. **3**, on the other hand, exhibited specific inhibition of CYP24A1, with substantial selectivity of 80 over CYP27B1. Further analysis revealed that **3** acts as a competitive inhibitor of both enzymes (Fig. 5) and that prolonged incubation with the enzymes did not exert extra inhibitory activity, suggesting that inhibition occurred instantly without substantial conformational changes in the proteins.

To confirm the inhibitory effect of **3** toward CYP24A1 in vitamin D responsive cells, we determined the half life of $1,25(OH)_2D_3$ in mouse osteoblast culture with and without a supplement of inhibitors. At high doses of $1,25(OH)_2D_3$ treatment (2.5 nM), the pool of residual $1,25(OH)_2D_3$ continuously decreased in the medium and eventually reached near depletion in 48 h, while $1,25(OH)_2D_3$ remained stable in the presence of **3** over the entire period (Fig. 6). The ability of **3** to sustain $1,25(OH)_2D_3$ in the mouse further demonstrated its effectiveness in CYP24A1 inhibition.

3.2.2. *In vitro and in vivo evaluations of 19-nor-1,25-$(OH)_2D_3$ analogs **2** and **3***

The newly synthesized 19-nor-1α,25-dihydroxyvitamin D_3 analogs were also exposed to a standard set of *in vitro* assays [28] to ascertain their effects on receptor binding, cell differentiation and gene transcription. As shown in Table 2, both **2** and **3** appeared to bind the VDR with lower affinity than the native hormone (**1**), with **2** also being very inactive in inducing both HL60 cell differentiation and transcription of 24-hydroxylase in rat osteosarcoma cells. Interestingly, **3** causes the differentiation of HL-60 cells with the same potency as $1,25(OH)_2D_3$ (**1**), whereas its transcriptional activity is markedly lower than $1,25(OH)_2D_3$ (**1**). Importantly, this cell type difference in biological potency was also observed *in vivo* where **3** (CPA-1), showed very little activity in bone, but was quite potent in stimulating calcium transport in the intestine (Fig. 7). In accordance to its reduced *in vitro* activity, **2** was also very inactive *in vivo* (data not shown).

3.3. Docking study

A molecular docking study was performed in order to rationalize the selectivity profile of compound **3** towards the hCYP24A1 isoenzyme, by comparing its ability to discriminate between the two isoenzymes of interest (hCYP24A1 and hCYP27B1). Indeed an optimal

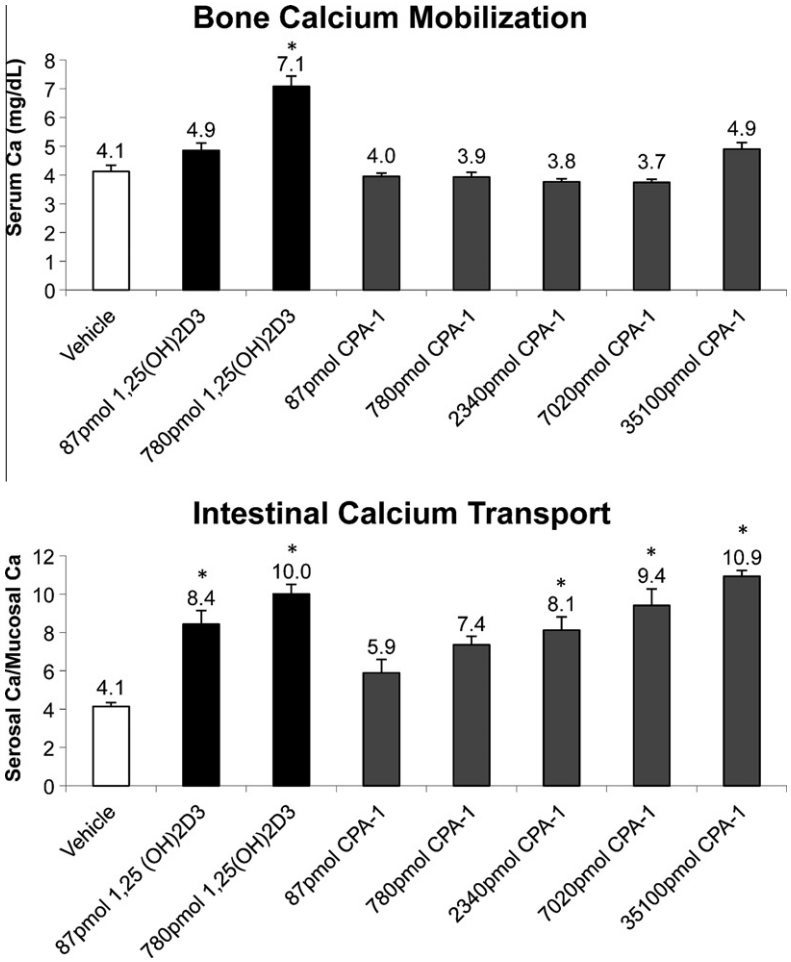

Fig. 7. Effects of $1,25(OH)_2D_3$ and compound **3** (CPA1) on bone calcium mobilization and intestinal calcium transport. Values shown are average ± SEM. Asterisks indicate values that are statistically different from Vehicle control ($p < 0.05$, Dunnett's).

Table 3
Relevant information coming from structural analysis of the natural ligands Calcitriol and Calcifediol docked into the sites of hCYP24A1 and hCYP27B1 isoenzymes respectively, and the compound **3** docked in the two isoenzymes.

Isoenzyme	Ligand	Interactions with the enzyme	H bonds	Orientation
hCYP24A1	Calcitriol	HEM520 HOH4 MET246 ALA326 GLU329 THR330 VAL391 PHE393 THR394 SER498 GLY499	MET246 GLU329	In agreement with the one reported in Ref. [39]
	3	HEM520 HOH4 LEU148 MET246 ALA326 GLU329 PHE393 HIS497 SER498 GLY499	HIS497	Calcitriol-like
	Calcifediol	HEM520 SER111 THR114 GLU115 ARG117 ARG118 LEU127 THR128 ALA224 VAL225 PHE229 LEU316 VAL384 ASN387	ASN387 ARG117	In agreement with the one reported in Ref. [40]
hCYP27B1		HEM520 CYS108 THR114 ARG117 LEU127 THR128 PHE221 ALA224 VAL225 VAL228 LEU233 PHE299 LEU316 SER388 ARG453 VAL494	–	Calcifediol Reverse

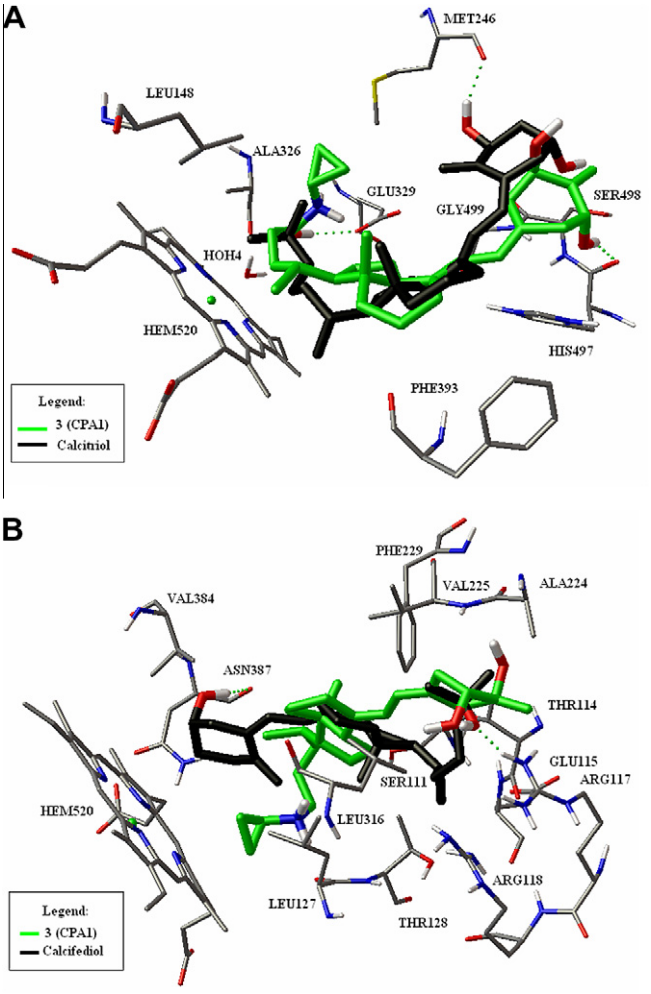

Fig. 8. (A) A comparison of docking results for analog **3** (CPA1) and the natural ligand Calcidiol ($1,25(OH)_2D_3$) in the model of hCYP24A1. Analog **3** is capable of docking the hCPA24A1 active site in the same general configuration as Calcidiol, with the side chain positioned over the heme. (B) A comparison of docking results for analog **3** (CPA1) and the natural ligand Calcifediol ($25(OH)D_3$) in the model of hCYP27B1. Analog **3** docked the hCYP27B1 active site with an orientation opposite to that of Calcifediol, thus preventing it's A-ring from interacting with the heme.

CYP24A1 inhibitor must inhibit CYP24A1 with minimal interference with the activity of CYP27B1. Therefore the possibility to bind according to orientations suitable for catalysis was investigated for compound **3** both in the hCYP24A1 and hCYP27B1 active sites.

To validate our theoretical models of compound **3** bound to the two isoenzymes and to help elucidate the molecular details that are important for secosteroid recognition, Calcitriol [$1,25(OH)_2D_3$, the natural ligand of CYP24A1] and Calcifediol [$25(OH)D_3$, the natural ligand of CYP27B1] were first docked within the binding site of their respective enzymes. Once the orientation and conformation of each ligand within the binding site were optimized by docking simulation, the best scoring pose was further relaxed and then analyzed to identify the most relevant interactions (Table 3).

We found that Calcitriol is engaged within the catalytic center of hCYP24A1 with its 25-hydroxylated side chain positioned over the heme. As shown in Fig. 8A, its conformation is stabilized by multiple hydrophobic contacts, and at least two hydrogen bonds (i.e., between the 1α-OH and MET246, and the 25-OH and GLU329). Notably, the residues involved in the interaction are the same as those suggested by other authors to be important for secosteroid binding and catalysis in rat models [39].

Calcifediol binds to the active site of hCYP27B1 in a configuration that positions the C-1 of the A-ring moiety toward the heme group [40]. Its conformation is also stabilized by two hydrogen bonds (i.e., between the 25-OH group and ARG117, and the 3β-OH with ASN387 (Fig. 8B).

Finally, compound **3** was docked within the binding site of the two isoenzymes using the same protocol as for the natural ligands, and the resulting theoretical models were analyzed to identify those features that enable this compound to discriminate between the two enzyme isoforms.

As depicted in Fig. 8A, compound **3** docks very well within the hCYP24A1 binding site, in a manner very similar to Calcitriol. Both

molecules (the substrate and the inhibitor) show contacts to the same enzyme residues (see Table 3) and have a similar orientation within the hCYP24A1 binding site, with the side chain positioned over the heme, thus allowing for catalysis.

On the other hand, our docking studies show that, whereas Calcifediol docks within the active site of hCYP27B1 in a configuration that positions the C-1 of the A-ring moiety toward the heme group of the hCYP27B1, thus allowing the catalysis, compound **3** takes an orientation not suitable for catalysis, projecting it's A-ring far away from the heme group (See Fig. 8B). Furthermore, no hydrogen bonds are observed between the ligand groups and the enzyme residues (Table 3).

These findings provide an explanation for the observed selectivity of compound **3** in inhibiting the human CYP24A1 versus human CYP27B1.

4. Discussion

CYP24A1 plays a key role in tuning the levels and function of $1,25(OH)_2D_3$; inhibition of CYP24A1 opens up a very wide field of possible applications ranging from basic research to the prevention and treatment of diseases. There is general agreement that unbalanced high and/or long-lasting expression of CYP24A1 can contribute to the pathology of diseases that otherwise would respond to endogenous or supplement vitamin D in a favorable way like chronic kidney disease, bone disease, cancers, and psoriasis. In these cases, inhibition of CYP24A1 could be the appropriate strategy to increase the lifetime and thereby the function of vitamin D. In this work, we showed that Azole-type (**2**) and cyclopropylamine (**3**) derivatives of 2-methylene-19-nor-1α,25-dihydroxyvitamin D_3 are very potent CYP24A1 inhibitors. Consistent to what has been reported in literature for others azole-type CYP inhibitors, the imidazole side chain modified analog **2** displayed only a moderate selectivity toward CYP24A1 over CYP27B1 while being basically inactive as a $1,25(OH)_2D_3$ analog. On the other hand, the introduction of a cyclopropylamino group on the side chain of 2-methylene-19-nor-1a,25-dihydroxyvitamin D_3 proved to be a good strategy at producing $1,25(OH)_2D_3$ analogs with desirable physiological characteristics. In fact, **3** combined the ability to specifically inhibit CYP24A1, thus preventing 24-hydroxylation of $1,25(OH)_2D_3$ and extending the hormone half life *in vitro*, with a potency to induce differentiation of human promyelocytic leukemia HL-60 cells, and showing lower potency in raising calcium tissue levels. Therefore, this new cyclopropylamine entity **3**, shows promise to be used either alone or in combination with other chemotherapeutic agents in the treatment or prevention of specific types of cancer.

A molecular docking study was also performed to rationalize the selectivity profile of **3** towards the CYP24A1 isoenzyme. It was found that **3** docked with high affinity to human CYP24A1 (Energy −8.18 kcal/mol) with an orientation that is highly similar to Calcitriol, with the side chain positioned in close proximity to the heme group (Fig. 8A). In particular, the binding of **3** within the active site is stabilized by a hydrogen bond between the 3β-OH and His497, and multiple hydrophobic interactions with key conserved residues (Table 3). However, compound **3** did not show noticeable turnover under experimental conditions in the inhibition assay [27], suggesting that a longer and bulkier side chain may impair CYP24A1's ability to acquire the closed form needed for catalysis, and simply enabling the compound to compete with the natural substrate for the binding pocket. These insights correlate well with previous observations that CYP24A1 requires a hydroxyl group at C25 to introduce the C24 vicinal hydroxyl group [39].

On the other hand, when compound **3** is complex with CYP27B1, its orientation within the active site (Fig. 8B) is not a good mimic for Calcifediol with respect to the position of the A ring relative to the heme prosthetic group, thus reducing the ability of compound **3** to compete with the natural ligand for the binding pocket.

Taken together, these results are in agreement with our experimental data that shows that **3** is approximately 80 times more selective towards inhibiting CYP24A1 over CYP27B1.

Unlike what has been described for many cyclopropylamine-based inhibitors, time-dependent and irreversible inactivation was not observed for our cyclopropylamine analog **3**, which instead acted as a competitive inhibitor (Fig. 5). To this end, it is interesting to note that when we docked **3** into the binding site of the human CYP24A1, we observed that the distance between the Fe^{3+} and the α-carbon of the cyclopropylamino group was 7.3 Å. Such a great distance would not favor either the α-hydroxylation or single electron transfer cyclopropane-ring opening, which are considered the most accredited mechanisms for cyclopropylamine suicidal inactivation of cytochrome P-450 enzymes [41].

Ongoing studies in our laboratory are directed toward optimizing the lead structure with respect to specificity, selectivity, efficacy and absence of toxicity in appropriate model systems. If successful these studies can result in compounds suitable to enter pre-clinical and clinical drug development programs.

Acknowledgments

The work was supported in part by funds from the Wisconsin Alumni Research Foundation. We gratefully acknowledge Jean Prahl, and Jennifer Vaughan, for carrying out the *in vitro* studies, and Erin Gudmundson for conducting the *in vivo* studies. We thank Dr. Mark Anderson for his assistance in recording NMR spectra. This study made use of the National Magnetic Resonance Facility at Madison, which was supported by the NIH Grants P41RR02301 (BRTP/NCRR) and P41GM66326 (NIGMS). Additional equipment was purchased with funds from the University of Wisconsin, the NIH (RR02781 and RR08438), the NSF (DMB-8415048, OIA-9977486, and BIR-9214394), and the US Department of Agriculture. The authors gratefully acknowledge and wish to extent their deep appreciation to Prof. Aldo Balsamo for critically reviewing this manuscript.

References

[1] Deluca HF. Evolution of our understanding of vitamin D. Nutr Rev 2008;66:S73–87.
[2] Holick MF. The vitamin D deficiency pandemic and consequences for nonskeletal health: mechanisms of action. Mol Aspects Med 2008;29:361–8.
[3] Bikle D. Nonclassic actions of vitamin D. J Clin Endocrinol Metab 2009;94:26–34.
[4] Prosser DE, Jones G. Enzymes involved in the activation and inactivation of vitamin D. Trends Biochem Sci 2004;29:664–73.
[5] Eeln G, Gysemans C, Verlinden L, Vanoibeek E, De Clercq P, Van Haver D, et al. Mechanisms and potential of the growth inhibitory actions of vitaminD and analogs. Curr Med Chem 2007;14:1893–910.
[6] Jones G. Vitamin D and analogues. In: Bilezikian JP, Raisz LG, Martin TJ, editors. Principles of bone biology. Amsterdam: Elsevier Academic Press; 2008. p. 1777–99.
[7] Deeb KK, Trump DL, Johnson CS. Vitamin D signaling pathways in cancer: potential for anticancer therapeutics. Nat Rev Cancer 2007;7:684–700.
[8] Reinhardt TA, Horst RL. Ketoconazole inhibits self-induced metabolism of 1,25-dihydroxyvitamin D_3 and amplifies 1,25-dihydroxyvitamin D_3 receptor up-regulation in rat osteosarcoma cells. Arch Biochem Biophys 1989;272:459–65.
[9] Peehl DM, Seto E, Hsu JY, Feldman D. Preclinical activity of ketoconazole in combination with calcitriol or the vitamin D analogue EB 1089 in prostate cancer cells. J Urol 2002;168:1583–8.
[10] Ly LH, Zhao XY, Holloway L, Feldman D. Liarazole acts synergistically with 1α,25-dihydroxyvitamin D_3 to inhibit growth of DU 145 human prostate cancer cells by blocking 24-hydroxylase activity. Endocrinology 1999;140:2071–6.
[11] Schuster I, Egger H, Bikle D, Herzig G, Reddy GS, Stuetz A, et al. Selective inhibition of vitamin D hydroxylases in human keratinocytes. Steroids 2001;66:409–22.
[12] Schuster I, Egger H, Nussbaumer P, Kroemer RT. Inhibitors of vitamin D hydroxylases: structure–activity relationships. J Cell Biochem 2003;88:372–80.

[13] Yee SW, Simons C. Synthesis and CYP24 inhibitory activity of 2-substituted-3,4-dihydro-2H-naphthalen-1-one (tetralone) derivatives. Bioorg Med Chem Lett 2004;14:5651–4.
[14] Aboraia AS, Yee SW, Gomaa MS, Shah N, Robotham AC, Makowski B, et al. Synthesis and CYP24A1 inhibitory activity of N-(2-(1H-imidazol-1-yl)-2-phenylethyl)arylamides. Bioorg Med Chem 2010;18:4939–46.
[15] Posner GH, Crawford KR, Yang HW, Kahraman M, Jeon HB, Li H, et al. Potent, low-calcemic, selective inhibitors of CYP24 hydroxylase: 24-sulfone analogs of the hormone 1α,25-dihydroxyvitamin D_3. J Steroid Biochem Mol Biol 2004;89–90:5–12.
[16] Kahraman M, Sinishtaj S, Dolan PM, Kensler TW, Peleg S, Saha U, et al. Potent, selective and low-calcemic inhibitors of CYP24 hydroxylase: 24-sulfoximine analogues of the hormone 1α,25-dihydroxyvitamin D_3. J Med Chem 2004;47:6854–63.
[17] Hanzlik RP, Kishore V, Tullman R. Cyclopropylamines as suicide substrates for cytochromes P-450. J Med Chem 1979;22:759–61.
[18] Angelastro MR, Laughlin ME, Schatzman GL, Bey P, Blohm TR. 17β-(Cyclopropylamino)-androst-5-en-3β-ol, a selective mechanism-based inhibitor of cytochrome P45017α (steroid 17α-hydroxylase/C17–20 lyase). Biochem Biophys Res Commun 1989;162:1571–7.
[19] Shah MA, Trackman PC, Gallop PM, Kagan HM. Reaction of lysyl oxidase with *trans*-2-phenylcyclopropylamine. J Biol Chem 1993;268:11580–5.
[20] Njar VCO, Duerkop J, Hartmann RW. Novel 19-(cyclopropylamino)-androst-4-en-3,17-dione: a mechanism-based inhibitor of aromatase. J Enzyme Inhib 1995;10:47–56.
[21] Mitchell DJ, Nikolic D, Jang MH, van Breemen RB, Hille R, Silverman RB. Inactivation of C30A trimethylamine dehydrogenase by *N*-cyclopropyl-α-methylbenzylamine, 1-phenylcyclopropylamine, and phenylhydrazine. Biochemistry 2001;40:8523–30.
[22] Totah RA, Hanzlik RP. Non-oxidative decarboxylation of glycine derivatives by a peroxidase. J Am Chem Soc 2002;124:10000–1.
[23] Vintem APB, Price NT, Silverman RB, Ramsay RR. Mutation of surface cysteine 374 to alanine in monoamine oxidase A alters substrate turnover and inactivation by cyclopropylamines. Bioorg Med Chem 2005;13:3487–95.
[24] Polasek TM, Elliot DJ, Somogyi AA, Gillam EMJ, Lewis BC, Miners JO. An evaluation of potential mechanism-based inactivation of human drug metabolizing cytochromes P450 by monoamine oxidase inhibitors, including isoniazid. Br J Clin Pharmacol 2006;61:570–84.
[25] Chiellini G, Grzywacz P, Plum LA, Barycki R, Clagett-Dame M, DeLuca HF. Synthesis and biological properties of 2-methylene-19-nor-25-dehydro-1alpha-hydroxyvitamin D(3)-26,23-lactones–weak agonists. Bioorg Med Chem 2008;16(18):8563–73.
[26] Lythgoe B, Moran TA, Nambudiry MEN, Ruston S. Allylic phosphine oxides as precursors of conjugated dienes of defined geometry. J Chem Soc Perkin Trans I 1976:2386–90.
[27] Zhu J, Barycki R, Chiellini G, Deluca HF. Screening of selective inhibitors of 1α,25-dihydroxyvitamin D_3 24-hydroxylase using recombinant human enzyme expressed in *Escherichia coli*. Biochemistry 2010;49(49):10403–11.
[28] Glebocka A, Sicinski RR, Plum LA, Clagett-Dame M, Deluca HF. New 2-alkylidene 1α,25-dihydroxy-19-norvitamin D_3 analogues of high intestinal activity: Synthesis and biological evaluation of 2-(3′-alkoxypropylidene) and 2-(3′-hydroxypropylidene) derivatives. J Med Chem 2006;49:2909–20.
[29] Guex N, Peitsch MC. SWISS-MODEL and the Swiss-PdbViewer: an environment for comparative protein modeling. Electrophoresis 1997;18:2714–23.
[30] Berman HM, Westbrook J, Feng Z, Gilliland G, Bhat TN, Weissig H, et al. The Protein Data Bank. Nucleic Acids Res 2000;28:235–42.
[31] blast.ncbi.nlm.nih.gov/.
[32] Pieper U, Narayanan E, Davis FP, Braberg H, Madhusudhan MS, Rossi A, et al. MODBASE: a database of annotated comparative protein structure models and associated resources. Nucleic Acids Res 2006;34:291–5.
[33] Morris GM, Goodsell DS, Halliday RS, Huey R, Hart WE, Belew RK, et al. Automated docking using Lamarckian genetic algorithm and an empirical binding free energy function. J Comput Chem 1998;19:1639–62.
[34] Solis FJ, Wets RJB. Minimization by Random Search Techniques. Math Oper Res 1981;6:19–30.
[35] Grzywacz P, Chiellini G, Plum LA, Clagett-Dame M, Deluca HF. Removal of the 26-methyl group from 19-nor-1α,25-dihydroxyvitamin D_3 markedly reduces in vivo calcemic activity without altering in vitro VDR binding, HL-60 cell differentiation, and transcription. J Med Chem 2010;53(24):8642–9.
[36] Ley SV, Norman J, Griffith WP, Marsden SP. Tetrapropylammonium perruthenate, Pr_4NRuO_4, TPAP: a catalytic oxidant for organic synthesis. Synthesis 1994:639–66.
[37] Posner GH, Crawford KR, Peleg S, Welsh JE, Romu S, Gewirtz DA, et al. A non-calcemic sulfone version of the vitamin D(3) analogue seocalcitol (EB 1089): chemical synthesis, biological evaluation and potency enhancement of the anticancer drug adriamycin. Bioorg Med Chem 2001;9:2365–71.
[38] Sicinski RR, Prahl JM, Smith CM, Deluca HF. New 1alpha, 25-dihydroxy-19-norvitamin D_3 compounds of high biological activity: synthesis and biological evaluation of 2-hydroxymethyl, 2-methyl, and 2-methylene analogues. J Med Chem 1998;41:4662–74.
[39] Annalora AJ, Goodin DB, Hong WX, Zhang Q, Johnson EF, Stout CD. Crystal structure of CYP24A1, a mitochondrial cytochrome P450 involved in vitamin D metabolism. J Mol Biol 2010;396:441–51.
[40] Yamamoto K, Uchida E, Urushino N, Sakaki T, Kagawa N, Sawada N, et al. Identification of the amino acid residue of CYP27B1 responsible for binding of 25-hydroxyvitamin D_3 whose mutation causes vitamin D-dependent rickets type 1. J Biol Chem 2005;280:30511–6.
[41] Lee HB, Sung MJ, Blackstock SC, Cha JK. Radical cation-mediated annulation. Stereoselective construction of bicyclo[5.3.0]decan-3-ones by aerobic oxidation of cyclopropylamines. J Am Chem Soc 2001;123:11322–4.